applied sciences

MDPI

Article

Microstructural and Chemical Characteristics of Archaeological White Elm (*Ulmus laevis* P.) and Poplar (*Populus* spp.)

Amir Ghavidel [1], Reza Hosseinpourpia [2,*], Jana Gelbrich [3], Miklós Bak [4] and Ion Sandu [5,6,7]

1 Doctoral School of Geosciences, Alexandru Ioan Cuza University of Iasi, 700506 Iasi, Romania; amir.ghavidel@lnu.se
2 Department of Forestry and Wood Technology, Linnaeus University, Lückligs Plats 1, 351 95 Växjö, Sweden
3 Leibniz-IWT-Institute for Materials Testing, Paul-Feller Strasse 1, 28199 Bremen, Germany; gelbrich@mpa-bremen.de
4 Institute of Wood Technology and Technical Sciences, University of Sopron, 9400 Sopron, Hungary; bak.miklos@uni-sopron.hu
5 Institute of Interdisciplinary Research, Alexandru Ioan Cuza University of Iasi, 700506 Iasi, Romania; ion.sandu@uaic.ro
6 Academy of Romanian Scientists (AOSR), 54 Splaiul Independentei St., Sect. 5, 050094 Bucharest, Romania
7 Romanian Inventors Forum, Iasi, 3 Sf. Petru Movila Street, Bloc L11, Sc. A, Et. 3, Ap. 3, 700089 Iasi, Romania
* Correspondence: reza.hosseinpourpia@lnu.se; Tel.: +46-0470-70-80-74

Abstract: The degradation states of archaeological white elm, with an age estimation of ~350 years, and poplar, with an age approximation of ~1000–1200 years, were studied by means of different chemical and microscopy analyses. Recently cut samples from the respective species were used for comparison reasons. The chemical composition analysis of the archaeological samples showed significantly low holocellulose values, while the lignin, extractive, and ash contents were considerably high, as compared with the recently cut samples. The Fourier-transform infrared (FTIR) spectroscopy also confirmed the changes in the chemical structure of the archaeological elm and poplar samples. The light and scanning electron microscopies illustrated that the erosion bacteria were the main degrading agent in both archaeological elm and poplar, although the hyphae of rot fungi were detected inside the vessel elements of the archaeological poplar sample.

Keywords: archaeological wood; biological degradation; FTIR; light microscopy; SEM

Citation: Ghavidel, A.; Hosseinpourpia, R.; Gelbrich, J.; Bak, M.; Sandu, I. Microstructural and Chemical Characteristics of Archaeological White Elm (*Ulmus laevis* P.) and Poplar (*Populus* spp.). *Appl. Sci.* **2021**, *11*, 10271. https://doi.org/10.3390/app112110271

Academic Editor: Giuseppe Lazzara

Received: 29 September 2021
Accepted: 29 October 2021
Published: 2 November 2021

1. Introduction

Wood has played a significant role in human life. It is mainly composed of cellulose, hemicelluloses, and lignin polymers. In the biological life cycle, wood undergoes degradation when it is exposed to suitable conditions [1,2]. Factors such as solar radiation, oxygen, water, heat, wind-blown particles, pollution, and microorganisms cause inter- and intra-molecular breakage in wood polymers and thus degrade the wood structure. Solar radiation causes photochemical degradation on the wood surface by the decomposition of wood polymers, mainly lignin [3]. Depolymerization of lignin through photon absorption results in the production of free radicals that can penetrate deeper into the wood structure and cause further degradation under the surface layer [1,3]. Moisture content alteration induced by rainfall or water contact causes continuous swelling and shrinkage in the wood cell wall and thus enhances crack formation [4]. Although temperature is not as important as moisture content and solar radiation, the rate of photochemical, oxidative reactions, and wood decay increases at elevated temperatures [5–7].

As described previously, archaeological wood is defined as a dead wood that has been left by an extinct human culture in a specific natural environment, which may or may not have been changed for or by use [1]. Archaeologists use studies on archaeological wood to better understand the past of human technology in making wooden tools and using them in their lives. They collect remarkable archaeological woods from different

applicational conditions that are mostly degraded by different types of organisms, such as fungi, insects, bacteria, marine organisms, or weathering factors. Among others, the degradation of archaeological wood by fungi and bacteria is the most common [1]. The main wood decomposing fungi are white-rot, brown-rot, and soft-rot. White-rot fungi can simultaneously degrade all polymers in wood, or they can selectively degrade the lignin in wood. Simultaneous degradation of wood is the most common degradation type, and different fungal enzymes are involved to erode the wood cell walls from the lumen to the middle lamella [8], and they often cause bleaching of normal wood coloration [9]. The selective lignin degradation is performed by fungal enzymes to remove lignin and non-cellulosic polysaccharides without extensive degradation of cellulose [10]. This process is particularly useful for bio-pulping, biodegradation of recalcitrant materials, and other applications [11]. Brown-rot fungi degrade wood by the depolymerization of cellulose and hemicelluloses [12] and modification of the lignin structure mainly through demethoxylation and demethylation [13,14]. The mechanisms of brown-rot degradation have been extensively studied during the last decades, and it is commonly accepted that in the initial degradation stage enzymes cannot penetrate the micro-pores of the cell wall because of their large hydrodynamic volumes [15,16]. It is thus assumed that the incipient attack on crystalline cellulose is caused by hydroxyl radicals produced via the Fenton reaction [17–19]. Considerable losses in wood strength occur very early in the decay process and cubical cracks are the typical macroscopic pattern of brown-rot degraded wood [19]. Although brown-rot fungi commonly decay ancient and historic buildings [20], their activity becomes highly restricted in some terrestrial and aquatic environments, i.e., little oxygen exists in wood that is excessively wet or saturated with water or buried deep in sediments [19]. In contrast, soft-rot fungi are particularly active in soil, moist conditions, and under high preservative loading. Soft-rot degrades the wood structure either by forming diamond-shaped cavities aligned with the cellulose microfibril angle within the S2 cell wall layer or by more generalized degradation of the entire S2 cell wall layer from the lumen outward [21]. The middle lamella is not degraded by soft-rot but may be modified in advanced stages of decay. As decay progresses, extensive carbohydrate loss occurs, which results in large strength loss, and lignin concentrations increase in the residual wood [9]. They can be often found with wood-degrading bacteria. However, they can be differentiated by the remnants of degradation. Soft-rot fungi leave remnants of hyphae in the degradants, while bacteria usually cause granular structure debris [22–24].

Wood degrading bacteria have a higher tolerance against high wood extractive and lignin content, high preservative loading, and low levels of oxygen in the wood [25]. Three main groups of wood degrading bacteria, such as erosion, cavitation, and tunnelling bacteria, have been distinct [9]. Erosion bacteria degrade S2 wall layers by depleting the cellulose and hemicelluloses from the wood. The residual porous material consists of lignin from the S2 cell wall layers and compound middle lamellae. This bacteria type can degrade wood in anoxic or low oxygen level conditions [26–28]. Cavitation bacteria cause diamond-shaped or irregular cavities inside cell walls near a pit chamber or directly in the S2 cell wall layer. The cavities are oriented perpendicular to the long direction of the fibers [27]. Tunneling bacteria produce minute tunnels that occur in all areas of wood cell walls, including highly lignified middle lamellae [7]. They degrade all cell wall components and degrade/modify lignin to some minor extent [29,30].

The archaeological woods that have survived after hundreds and even thousands of years are extremely valuable resources and deserve careful attention, mainly due to their historical importance. In addition, determination of the degradation state in archaeological woods increases our knowledge of finding an appropriate method for excavation, transferring, storage, and preservation of these valuable elements through green protocols [31–33]. Therefore, the aim of this work is a contribution to understanding the changes in the chemistry and microstructure of archaeological wood induced by biotic agents by means of chemical composition analysis, Fourier-transform infrared (FTIR) spectroscopy, and light microscopy and scanning electron microscopy (SEM). Archaeological white elm

(*Ulmus laevis* P.), with an approximate age of 350 years, and poplar (*Populus* spp.), with an approximate age of 1000–1200 years, were selected for this study and the results were compared with those of recently cut samples.

2. Materials and Methods

2.1. Raw Materials

The recently cut elm (*Ulmus laevis* P.) and poplar (*Populus nigra* L.) samples, measuring 45 mm × 90 mm × 4000 mm (L × T × R) boards, were collected from the northern part of Iran, Caspian Hyrcanian mixed forest. The region is located in the southern part of the Caspian Sea in Iran and the western regions in the Republic of Azerbaijan. The defect-free samples (no knot, cracks, and reaction wood) were cut from heartwood. The moisture contents of both recently cut samples were 9.9%. The density of recently cut elm and poplar were, respectively, 516.2 kg/m^{-3} and 506.3 kg/m^{-3}.

The archaeological elm sample was part of a historical building in the city of Iasi, Romania. This specimen was a flooring element, and the building was built about 350 years ago. The house had been abandoned for a long time and most of it was destroyed. These samples were buried under the soil and were excavated during the excavation operation in September 2009. The type of soil was sand and gravel. The moisture content of the sample during analysis was 11.6%, and the density of the sample was 330.0 kg/m^{-3}.

The archaeological poplar sample was a part of a boat in the Moldavian region of Romania. The boat was buried in the Moldova riverbed. The sample was not waterlogged because the river had changed course over a long period, and the soil at the sample site had low moisture content. Thus, it is classified as dry archaeological wood. After the discovery of this boat, it was transferred to the history museum in the city of Iasi, and it was kept in storage at the museum for one year until the exhibition hall with proper conditions (50% RH and 18–20 °C) became ready. The sample was removed from the boat during the restoration process. The approximate age of this specimen is 1000 to 1200 years. The moisture content and the density of the sample during analysis were 10.5% and 288.5 kg/m^{-3}, respectively.

It should be noted that the ages of the archaeological wood samples were determined by the stratigraphic evaluation method [6,34]. The recently cut and archaeological specimens are shown in Figure 1. Both samples were chosen from the cracked-, knot-, and dust-free part of the wooden elements. A few millimeters of wood surfaces were removed carefully, and then the samples were cut randomly from the inner part of the subjects. The samples were not conserved with any chemicals. Since both archaeological specimens were found buried underground and in a dry environment, and the samples were found in their place of use, in their original context and undisturbed, the samples can be considered as a primary context group.

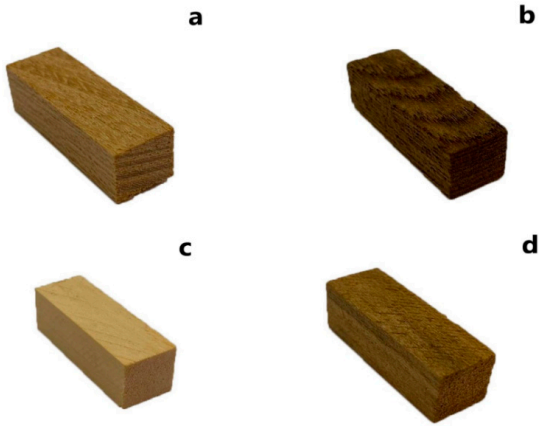

Figure 1. Recently cut (**a**) and archaeological elm (**b**) and recently cut (**c**) and archaeological poplar (**d**).

2.2. Evaluation Methods

2.2.1. Chemical Analysis

The chemical compositions of wood samples were analyzed according to Rowell 2012, [35], after milling with particle sizes of 250–425 µm. The moisture content of wood samples was detected using an Ohaus MB23 moisture analyzer [5,6]. The extraction content was determined on 2–3 g of oven-dried sample (at 103 °C for 24 h) using cyclohexane-ethanol (50:50 v/v) solution for 3 h. Then, the samples were oven-dried again and used for the assessment of holocellulose contents.

The holocellulose contents were determined by transferring the oven-dried samples to an Erlenmeyer flask, adding 80 mL of hot water (70 °C), 1 g of sodium chlorite, and 0.5 mL of acetic acid, keeping it for 6 h in a water bath at 70 °C. The same amounts of chemicals were added after every hour, and the flasks were gently shaken.

Ash content was determined according to EN 15403 standard [36]. About 2–3 g of oven-dried samples were placed in the dry ceramic dishes and transferred to the cold furnace. The temperature was set at 250 (±10) °C, and the samples were kept at this temperature for 50 min. Then, the temperature was increased to 550 (±10) °C, and the samples were kept for 1 h. Afterwards, samples were taken out, allowed to cool down in a desiccator, and were weighed. The lignin amount was calculated by subtracting from the sum of other components, i.e., by the sum of holocellulose, ash, and extractive contents. Each measurement was performed in triplicates, and the average value is presented.

2.2.2. Fourier-Transform Infrared (FTIR) Spectroscopy

The chemical structure of archaeological and recently cut wood samples was analyzed with ATR–FTIR spectroscopy (Perkin Elmer Frontier, Waltham, MA, USA) using a Bruker Invenio R spectrometer fitted with a diamond ATR unit. The ATR–FTIR spectra were recorded in the range of 4000 and 400 cm^{-1} at room temperature, averaging 64 scans with a resolution of 4 cm^{-1}. Three measurements were performed for each sample, and the average spectra were analyzed. The lignin index (*LI*) was calculated by lignin intensity at 1505 cm^{-1} and CH/CH_3 groups at 1375 cm^{-1} [31] using Equation (1):

$$LI = [\frac{I_{1505\ cm^{-1}}}{I_{1375\ cm^{-1}}}] \quad (1)$$

2.2.3. Light Microscope

For light microscopy, the samples were prepared according to a method described previously [5]. In brief, a thin transverse was cut by hand using a razor blade. During sectioning, the test fragments were retained in wet conditions. The sections were stained with 0.1% safranin and then washed with 50% ethanol. The sections were left in ethanol for 15 s and directly washed with distilled water, mounted on a microscope slide and covered with a coverslip. A high-definition color cooled DS-Fi1c camera and a Nikon ECLIPSE E600 microscope fitted with NIS-Elements (Nikon, Tokyo, Japan) tech were used to image the sections. Polarized light was used for observation of the tangential sections.

2.2.4. Scanning Electron Microscope (SEM)

A Hitachi S-3400N (Hitachi, Tokyo, Japan) device was used to analyze the microstructure of recently cut and archaeological wood samples, at a 30 Pa vacuum and an 8 kV accelerating voltage using a BSE detector. The working distance was 10 mm. The samples with the size of 5 × 5 × 5 mm^3 were sectioned with a razor blade. Three sections were prepared from each sample type and direction. The surfaces were not coated with a sputter coater before imaging, as described previously [6].

2.2.5. Statistical Analysis of the Results

Statistica 13.0 (StatSoft) software was used to evaluate the normal distribution and to perform the one-way analysis of variance (ANOVA) on the results of chemical analyses at a

95% confidence interval ($p < 0.05$). The statistical differences between values were assessed by Fisher's LSD test.

3. Results and Discussion

3.1. Chemical Analysis

The chemical compositions of recently cut and archaeological wood samples are shown in Table 1. As can be seen, the amounts of holocelluloses in recently cut elm and poplar were, respectively, 80.01% and 81.46%, while these amounts were significantly lower in archaeological elm and poplar, which were 56.45% and 51.18%, respectively. The amount of holocelluloses in hardwood species are generally between 59% to 85%, and it changes considerably at different tree age and growing location [34]. The reduction of holocellulose content in archaeological wood samples was widely reported previously [34,35,37–39]. It can be due to the degradation of polysaccharides at the initial stage of the ageing process [6,34,40]. The amount of lignin in the archaeological samples was significantly higher than in the recently cut samples, which is mainly attributed to the loss of other wood compounds, e.g., holocelluloses [1,6,41]. The extractive content of the archaeological elm and poplar were 2.50% and 3.55%, respectively, while these values for the recently cut samples were 1.26% and 1.48%, respectively. This significant difference can be due to the breakdown of wood polysaccharides into leachable monosaccharides or oligosaccharides during degradation processes [3,4]. Similar results were reported previously by Crestini et al. [42] for archaeological cypress wood. The ash contents in archaeological elm and poplar were 4.70% and 3.18%, respectively, and the recently cut samples showed a respective ash content of 0.65% and 0.61 for the elm and poplar samples. The differences were statistically significant (ANOVA, $p < 0.05$). There is a significantly higher amount of ash content in the archaeological wood samples. The deposition of inorganic elements in the wood structures during the service life and storage periods might be an additional reason. These findings are almost in agreement with the previous studies on the chemical compositions of archaeological oak and elm wood samples [43–46].

Table 1. Chemical compositions of recently cut and archaeological elm and poplar (wt%).

Wood Samples	Holocellulose	Lignin	Extractive	Ash
Recently cut elm	80.01 (±1.12) [a]	17.90 (±0.56) [a]	1.26 (±0.03) [a]	0.65 (±0.01) [a]
Archaeological elm	56.45 (±1.92) [b]	34.24 (±0.42) [b]	2.50 (±0.12) [b]	4.70 (±0.35) [b]
Recently cut poplar	81.46 (±2.00) [a]	14.66 (±0.05) [a]	1.48 (±0.42) [a]	0.61 (±0.04) [a]
Archaeological poplar	51.18 (±1.70) [b]	40.22 (±0.30) [b]	3.55 (±0.43) [b]	3.18 (±0.04) [b]

Values labelled with the small letters show the statistical differences between recently cut and archaeological specimens (ANOVA, Fisher's LSD test, $p < 0.05$).

FTIR spectroscopy was used to analyze the changes in the chemical structure of archaeological wood samples due to the storage and ageing process. Figure 2a,b illustrates the FTIR spectra of recently cut and archaeological elm and poplar wood samples. The absorption band between 3300 and 3400 cm^{-1} was assigned to the stretching vibration of the –OH group [5,46,47]. This band was identical in both recently cut and archaeological elm samples, while it was slightly decreased in the archaeological poplar. The stretching vibration in the region between 2800 to 3000 cm^{-1} is associated with the –CH group in cellulose, hemicellulose, and lignin [5,43]. The band at 1733 cm^{-1}, which is assigned to the stretching vibrations of the unconjugated C=O group and specific moieties, such as esters, had disappeared in the archaeological elm and poplar. This could be related to the strong degradation of hemicelluloses after the ageing process [41,45,48]. Both archaeological elm and poplar samples exhibited considerably higher absorption in the region between 1235 and 1646 cm^{-1}. These vibrations were mostly attributed to the stretching of the C=C and C=O groups in the lignin structure [6,49]. The *LI* values in both archaeological elm and poplar were strongly increased, i.e., from 0.71 and 0.82 in recently cut elm and poplar to the respective values of 1.67 and 1.40 in the archaeological samples. Similar results were

reported by Cavallaro et al. [31]. The bands at 1156, 1158, and 1029 cm^{-1} correspond to the vibrations of the C-O and C-C groups, i.e., the glycoside symmetric vibrations of C-O and C-C and the asymmetrical stretch of C-O and C-C [5,6,50]. The stretching band at 897 cm^{-1} was assigned to an in-plane symmetric vibration of C-H in cellulose [40,51], which was slightly increased in both archaeological samples. The chemical composition and FTIR analyses of archaeological elm and poplar samples illustrated a strong degradation of polysaccharides, which might be due to the microbial degradations. Pedersen et al. [40] revealed that bacterial degradation, e.g., erosion bacteria, cause significant degradation in holocelluloses. Therefore, brown-rot or soft-rot fungi and/or other microbial degrading agents such as bacteria might have been involved in the degradation of the archaeological elm and poplar samples.

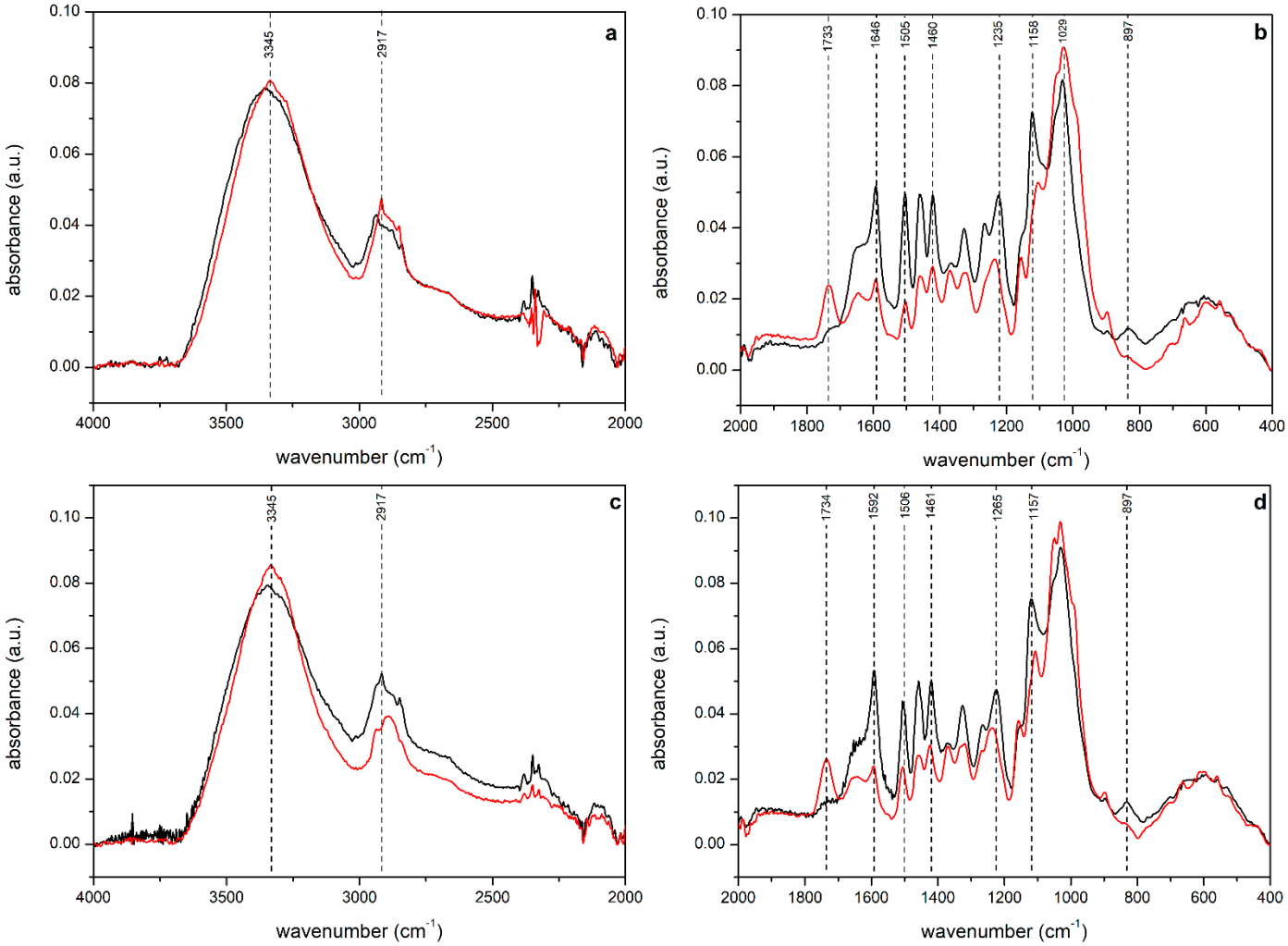

Figure 2. Fourier-transform infrared spectroscopy (FTIR) spectra of recently cut and archaeological elm (**a**,**b**) and poplar (**c**,**d**) in the region of 4000–2000 cm^{-1} and 2000–400 cm^{-1}. Red lines are for recently cut samples and black lines are for archaeological samples.

3.2. Morphological Decay Pattern

The identification of degradation patterns in most archaeological wood is based on their distinct decay patterns left behind like fingerprints due to the absence of the active degrading agents. Therefore, the characteristic troughs that are seen in the degraded cell walls are a particular distinguishing feature [1]. The microstructure of the archaeological elm and poplar samples was evaluated by means of light and scanning electron micro-

scopies. The light microscopy analyses of the recently cut and archaeological elm and poplar samples are presented in Figures 3 and 4.

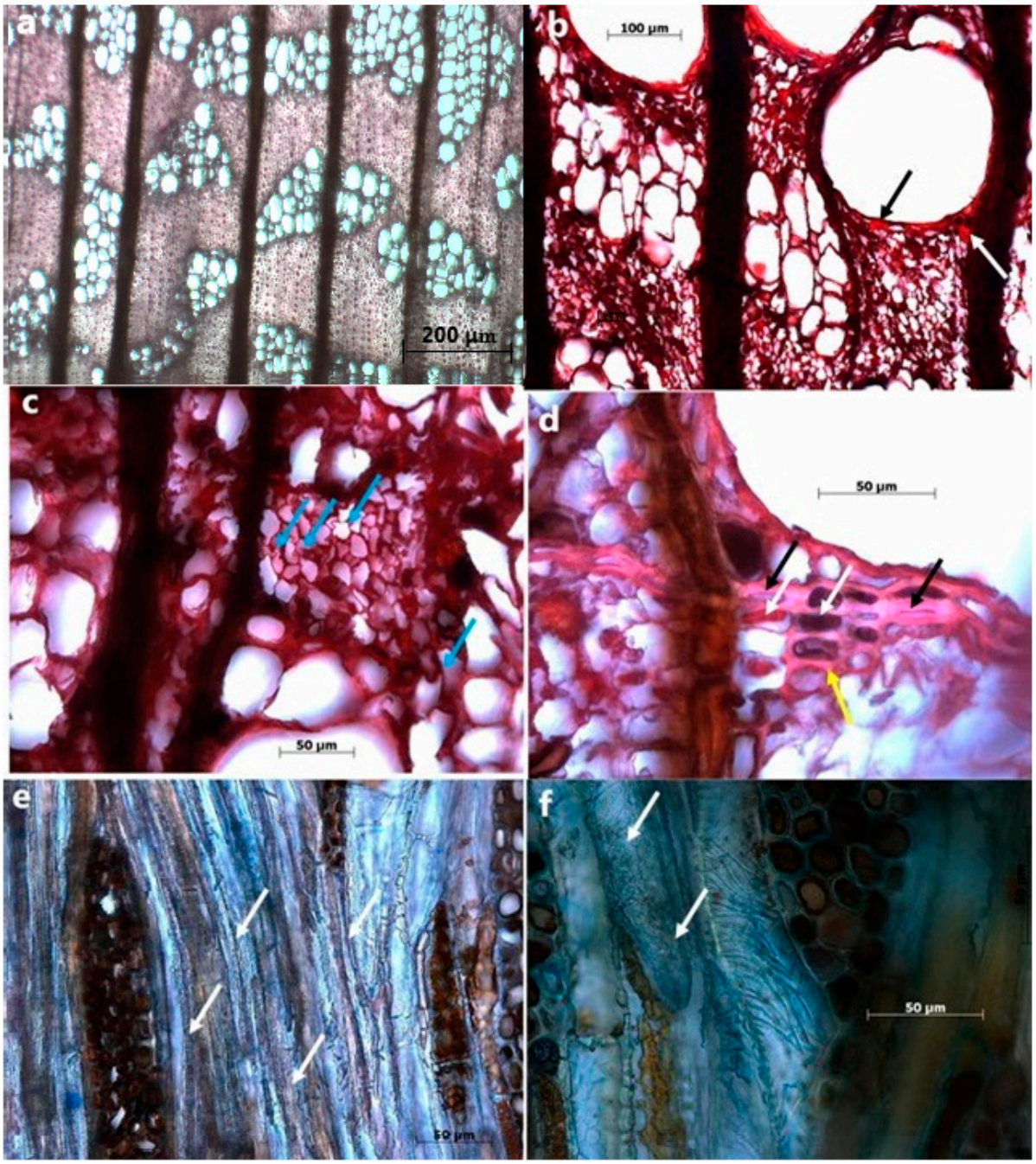

Figure 3. Light microscopy of cross-sections of recently cut (**a**) and archaeological elm (**b**–**d**) and from tangential section of archaeological elm using polarized light (**e**,**f**). Arrows indicate the damaged parts of archaeological wood samples.

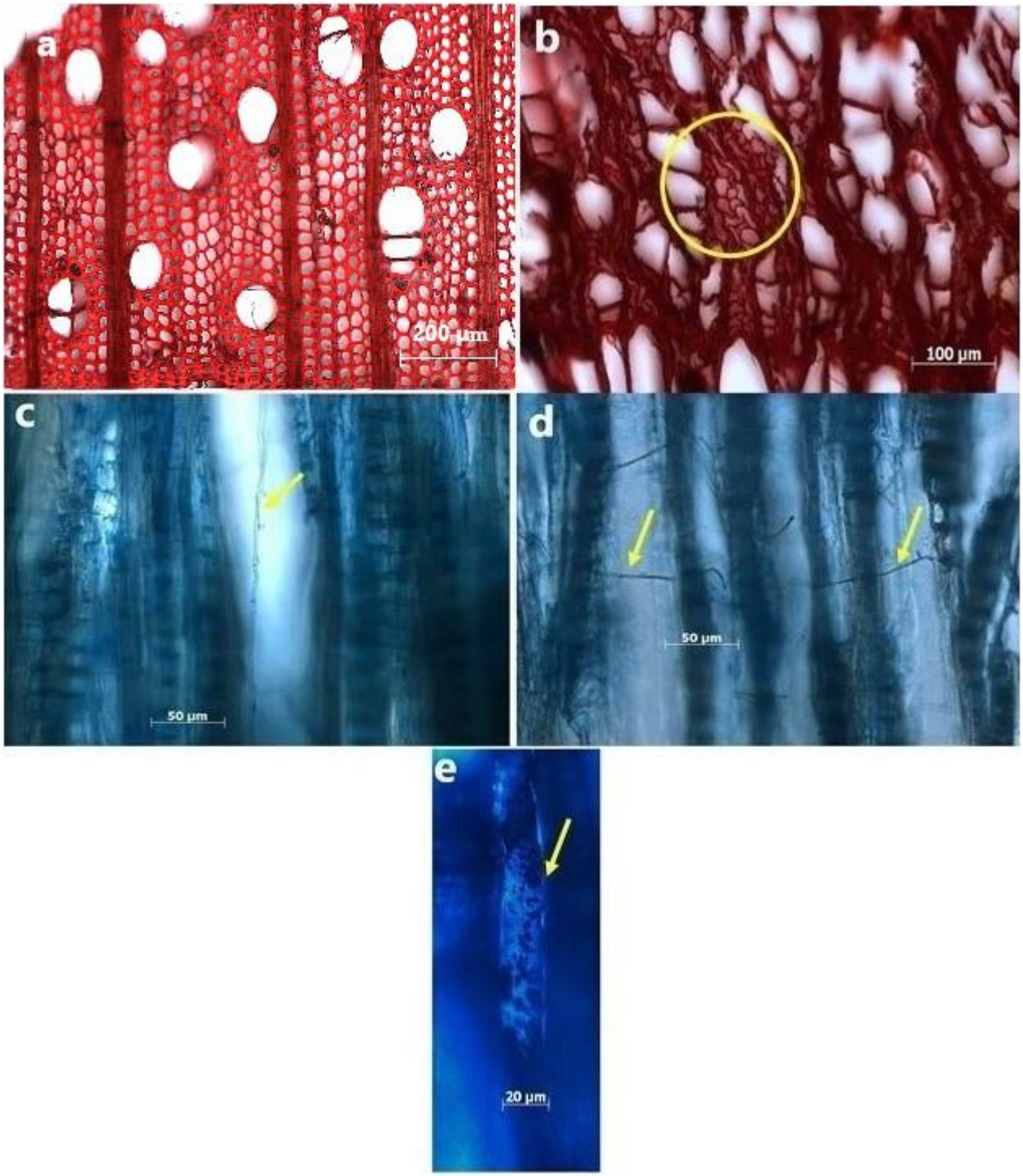

Figure 4. Light microscopy of cross-sections of recently cut (**a**) and archaeological poplar (**b**) and from tangential section of archaeological elm using polarized light (**c**–**e**). Arrows indicate the fungal hyphae (**c**,**d**) and bacterial degradation patterns (**e**) of archaeological wood samples.

As compared with the recently cut sample (Figure 3a), extensive degradations were observed in the cross-section of the archaeological elm (Figure 3b–d). Only a few cells, i.e., particularly those cells at the annual ring boundary area, look intact (black arrows in Figure 3b,d). The degradation occurred from the lumen towards the ML (yellow arrow in Figure 3d), and the residual materials were left in the lumen (white arrows in Figure 3d). The middle lamellas remained intact in terms of degradation, but in some cases began to collapse (blue arrows in Figure 3c) due to stress, e.g., cutting process for sample

preparation. This degradation pattern is typically associated with erosion bacteria degradation [21,37,40,46,52]. The fine degradation pattern of bacteria was also found as grainy structures in the tangential section (white arrows in Figure 3e,f). No fungal hyphae were detected in the cross and tangential sections, and thus it is assumed that the archaeological elm was mainly degraded by erosion bacteria.

Evidence of degradation by erosion bacteria means that the wood must have been stored for a long time under water-saturated, low-oxygen, or even oxygen-free conditions [1,53,54]. The fact that no fungal hyphae were found does not mean that fungi did not also decompose the wood, but probably in a relatively short time window before the conditions shifted in favor of the bacteria. Otherwise, fungal degradation patterns or hyphae would still be detectable.

The buried storage conditions of this archaeological elm wood seem to have changed very quickly to dry conditions. The gravelly, sandy soil suggests the possibility that the water was able to drain away quickly. It can also be assumed that the wood dried very quickly afterwards, as otherwise traces and hyphae of fungus would have been found.

The cross-section investigation of recently cut and archaeological poplar showed that the wood cells were highly degraded (Figure 4a,b), while the MLs stayed intact in the archaeological sample (Figure 4b). The collapse of the residual cell wall, mainly just the ML, (Figure 4b circle) is based on the reaction of stress by reduced strength. This could be pictured evidence of a brown-rot attack in the cross-sections. Fungal hyphae were not detected in the cross-section of archaeological poplar, but they were obviously shown in the tangential sections (Figure 4c–e). The direction of the fungal hyphae does not follow any particular orientation, as they are extended through the cells tangentially. The degradation pattern, e.g., the intact MLs and unspecific orientation of fungal hyphae, suggests that white-rot and soft-rot fungi seemed not to be involved in the decomposition of this archaeological poplar [21,49]. The hyphae observed in the sections are present only in cell lumina and colonize adjacent cells passing through the pits. This clearly indicates that these fungi are not ligninolytic or are less so. Some brown-rot fungi can only change the lignin structure [55,56] and could therefore also fall under this category. Unfortunately, no clear evidence for a brown-rot infestation could be found. It is also possible that the hyphae have colonized the wood only after salvage, e.g., due to inadequate proper storage. A trace of bacterial degradation was observed in a single cell of the tangential section with the help of polarized light (Figure 4e), by showing the rhombic-shaped cell wall losses. This degradation pattern is a typical sign of erosion bacteria in wood from wet and near-anaerobic environments, e.g., waterlogged archaeological wood and foundation piles [9,21,22,29,55].

As it was observed by light microscopy, the SEM micrographs of the archaeological elm also confirmed that the severe degradations occurred in wood cells (Figure 5a), although no evidence of fungal hyphae was found. The cells were mainly degraded, and no sound cell was found in the cross and tangential sections, which might be due to the shrinkage of the sample during the drying process [50]. This might be related to the deformation of cells during sectioning. The residual degradation materials in the cell lumens are obvious in Figure 5b,c (blue arrow). Grainy structures, as a sign of bacterial erosion, are visible in the ray parenchyma cells (white arrow in Figure 5c and blue arrow in Figure 5d). The ray parenchyma contains a higher quantity of sugars in comparison with fibers and vessels, as they are part of the nutrient reserves of the trees [21], and it is expected that those cells are susceptible to various degrading agents. Very recently, Cha et al. [56] revealed that the degradation of the parenchymal cell wall is delayed relative to its adjacent tracheas when they are exposed to erosion bacteria. However, it did not exhibit entire resistance to bacterial decay. The degradation patterns of the archaeological elm illustrated that the erosion bacteria were the main degrading agent. Although it was assumed that the fungi might have been involved in the degradation, i.e., according to the results obtained from chemical analysis, there were no fungal hyphae detected by microscopical analyses to approve it.

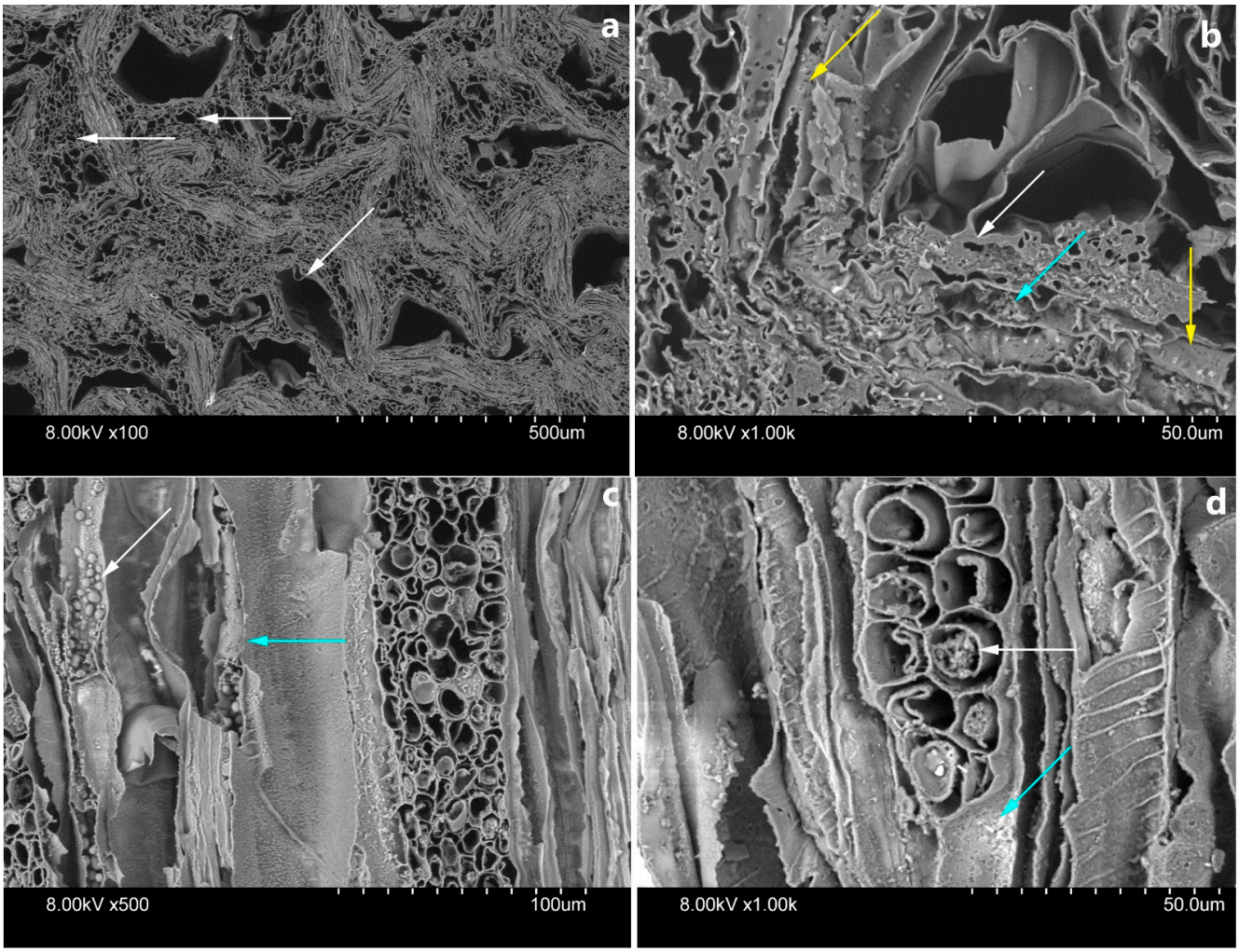

Figure 5. Scanning electron microscopy (SEM) micrographs from cross-sections (**a**,**b**) and tangential section (**c**,**d**) of archaeological elm. Arrows indicate the damaged parts of archaeological wood samples.

The scanning electron microscopy (SEM) micrographs of archaeological poplar are shown in Figure 6a–d. These images clearly illustrate the high degree of degradation and deformed cell walls, as indicated by white arrows. The hyphae are obvious in the cell lumens penetrating through the cells (blue arrow in Figure 6a). As observed by the light microscope, the SEM micrograph of the cross-section with higher magnification also showed that the MLs are intact (Figure 6b, blue arrows). The tangential section of archaeological poplar demonstrated that, despite the degradation of the cell structure, the intercellular pits (white arrow in Figure 6c) and perforation plates (blue arrow in Figure 6c) are still clearly visible. The grainy structured residues, a typical pattern of bacterial degradation [38], were found on the outer part of the cells (yellow arrow in Figure 6b). The hyphae, which are penetrating through the vessels (yellow and white arrows in Figures 6c and 6d, respectively), and grainy structured residues are also obvious in the tangential section (blue arrow in Figure 6d). Investigation of the morphological decay pattern together with the chemical analyses confirmed that the degradation in the archaeological poplar was most likely due to erosion bacteria. The main degradation might have occurred by erosion bacteria, due to the existence of the archaeological poplar in an aquatic environment with little oxygen exposure, as it was a part of a boat in a freshwater lake or river. The presence of fungi hyphae can be attributed to the improper storage and conservation condition in the museum.

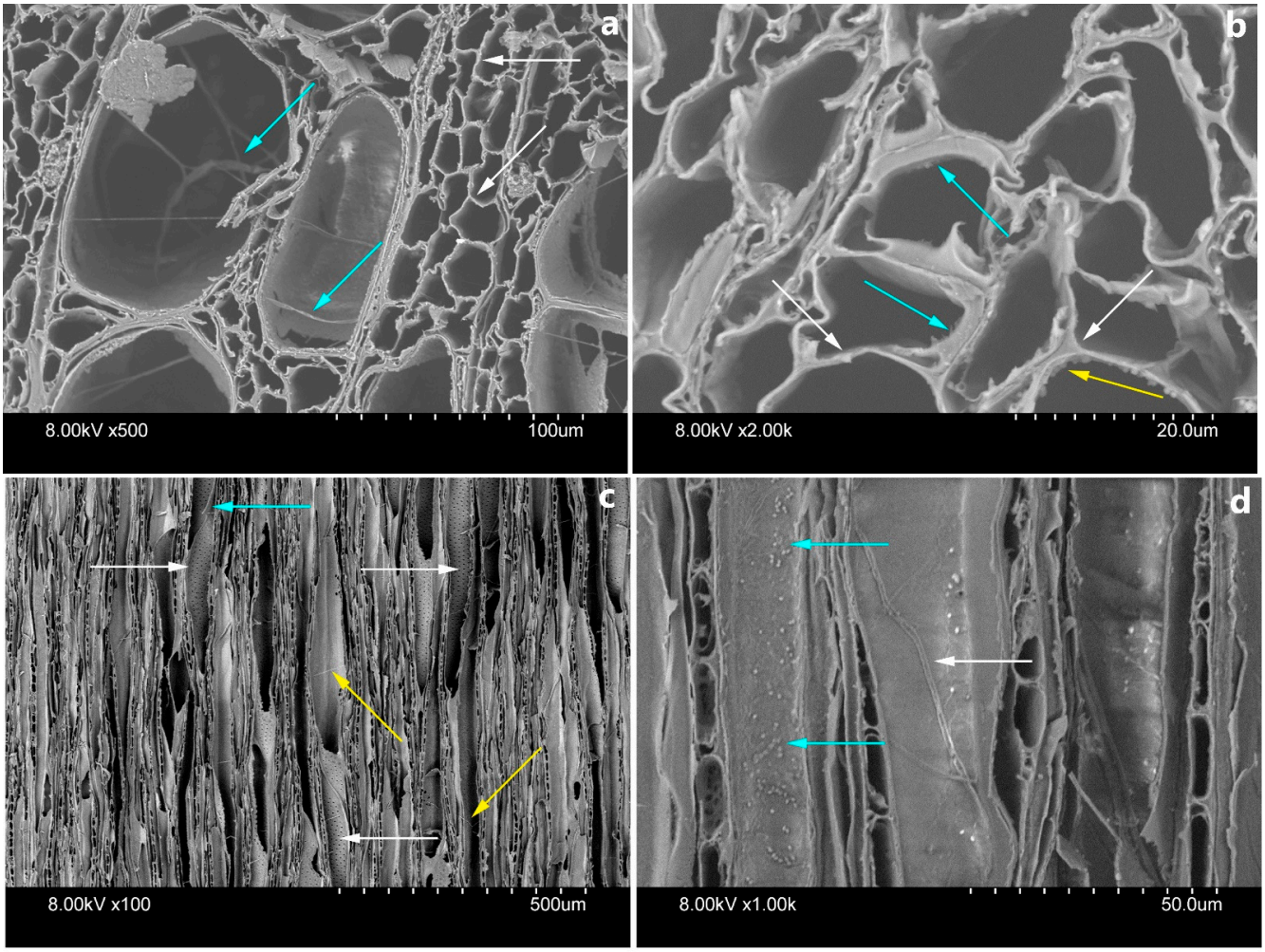

Figure 6. Scanning electron microscopy (SEM) micrographs of cross-sections from archaeological poplar (**a**,**b**) and tangential sections (**c**,**d**). Arrows indicate the damaged parts of archaeological wood samples.

4. Conclusions

Noticeable differences were observed in the chemical and anatomical structures of archaeological white elm (*Ulmus laevis* P.) and poplar (*Populus* spp.), as compared with the recently cut samples. FTIR and chemical composition analyses illustrated the strong degradation of polysaccharides, e.g., hemicelluloses and cellulose, in the archaeological samples, while the lignin content was higher than the recently cut samples. This, together with the microscopy examinations of decay patterns and residues, confirmed that the erosion bacteria were mainly involved in the degradation processes of both archaeological elm and poplar. The presence of fungi hyphae in the archaeological poplar is expected to be related to improper storage and conservation in the museum. The findings of this study suggest that the archaeological wood elements should be handled very carefully during excavation, transferring, and storage, as they still can be attractive for biotic agents. It is known that the degradation rate of the wood depends on the aggressiveness of environmental factors and how it is used in anthropogenic activities, with high or moderate risk. The study of archaeological species allows for obtaining data that can served as a reference for other studies.

Author Contributions: Conceptualization, A.G., R.H.; methodology, A.G. and R.H.; validation, A.G. and I.S.; investigation, A.G., J.G. and M.B.; resources, A.G., R.H. and I.S.; writing—original draft preparation, A.G. and R.H.; writing—review and editing, all authors. All authors have read and agreed to the published version of the manuscript.

Funding: This research received no external funding.

Institutional Review Board Statement: Not applicable.

Informed Consent Statement: Not applicable.

Data Availability Statement: Date of the compounds are available from the authors.

Conflicts of Interest: The authors declare no conflict of interest.

References

1. Björdal, C.G. Waterlogged Archaeological Wood, Biodegradation and Its Implications for Conservation. Ph.D. Thesis, Swedish University of Agricultural Science, Uppsala, Sweden, 2000.
2. Eriksson, K.E.; Johnsrud, S.C. Mineralization of carbon. In *Experimental Microbial Ecology*; Burns, R.G., Slater, J.H., Eds.; Blackwell: London, UK, 1982; pp. 134–153.
3. Kranitz, K.; Sonderegger, W.; Bues, C.-T.; Niemz, P. Effects of aging on wood: A literature review. *Wood Sci. Technol.* **2016**, *50*, 7–22. [CrossRef]
4. Hosseinpourpia, R.; Adamopoulos, S.; Mai, C. Effects of acid pre-treatments on the swelling and vapor sorption of thermally modified Scots pine (*Pinus sylvestris* L.) wood. *BioResources* **2018**, *13*, 331–345. [CrossRef]
5. Ghavidel, A.; Gelbrich, J.; Kuqo, A.; Vasilache, V.; Sandu, I. Investigation of Archaeological European White Elm (*Ulmus laevis*) for Identifying and Characterizing the Kind of Biological Degradation. *Heritage* **2020**, *3*, 1083–1093. [CrossRef]
6. Ghavidel, A.; Hofmann, T.; Bak, M.; Sandu, I.; Vasilache, V. Comparative Archaeometric Characterization of Recent and Historical Oak (*Quercus* spp.) Wood. *Wood Sci. Technol.* **2020**, *54*, 1121–1137. [CrossRef]
7. Feist, W.C. Outdoor Wood Weathering and Protection. In *Archaeological Wood: Properties, Chemistry, and Preservation*; Rowell, R.M., Barbour, R.J., Eds.; American Chemical Society: Washington, DC, USA, 1990; pp. 263–298.
8. Kirk, T.K.; Cullen, D. Enzymology and molecular genetics of wood degradation by white-rot fungi. In *Environmentally Friendly Technologies for the Pulp and Paper Industry*; Young, R.A., Akhtar, M., Eds.; John Wiley & Sons, Inc.: New York, NY, USA, 1998; pp. 273–308.
9. Blanchette, R.A. A review of microbial deterioration found in archaeological wood from different environments. *Int. Biodeterior. Biodegrad.* **2000**, *46*, 189–204. [CrossRef]
10. Ferraz, A.; Córdova, A.M.; Machuca, A. Wood biodegradation and enzyme production by Ceriporiopsis subvermispora during solid-state fermentation of Eucalyptus grandis. *Enzym. Microb. Technol.* **2003**, *32*, 59–65. [CrossRef]
11. Koike, K.; Itakura, S.; Enoki, A. Degradation of wood and enzyme production by Ceriporiopsis subvermispora Author links open overlay panel Hiromi Tanaka. *Enzym. Microb. Technol.* **2009**, *45*, 384–390.
12. Cowling, E.B. *Comparative Biochemistry of the Decay of Sweet-Gum by White- and Brown-Rot Fungi*; USDA Technical Bulletin; USDA: Washington, DC, USA, 1961.
13. Kirk, T.K. Effects of a brown-rot fungus, Lenzites frabea, on lignin in spruce wood. *Holzforschung* **1975**, *29*, 99–107. [CrossRef]
14. Eriksson, K.E.; Blanchette, R.A.; Ander, P. *Microbial and Enzymatic Degradation of Wood and Wood Components*; Springer Series in Wood Science; Springer: Berlin, Germany, 1990; p. 407.
15. Cowling, E.B.; Brown, W. Structural features of cellulosic materials in relation to enzymatic hydrolysis. *Adv. Chem. Ser.* **1969**, *95*, 152–187.
16. Flournoy, D.S.; Kirk, T.K.; Highley, T.L. Wood decay by brown-rot fungi: Changes in pore structure and cell wall volume. *Holzforschung* **1991**, *45*, 383–388. [CrossRef]
17. Koenigs, J.W. Production of extracellular H_2O_2 and peroxidase by brown rot fungi. *Phytopathology* **1972**, *62*, 100–110. [CrossRef]
18. Highley, T.L. Requirements for cellulose degradation by a brown-rot fungus. *Mater. Org.* **1977**, *12*, 25–36.
19. Green, F.; Highley, T.L. Mechanism of brown-rot decay: Paradigm or paradox. *Int. Biodeterior. Biodegrad.* **1997**, *39*, 113–124. [CrossRef]
20. Jennings, D.H.; Bravery, A.F. *Serpula Lacrymans: Fundamental Biology and Control Strategies*; Wiley: New York, NY, USA, 1991; 217p.
21. Goodell, B.; Winandy, J.E.; Morrell, J.J. Fungal Degradation of Wood: Emerging Data, New Insights and Changing Perceptions. *Coatings* **2020**, *10*, 1210. [CrossRef]
22. Singh, A.P.; Hedley, M.E.; Page, D.R.; Han, C.S.; Atisongkroh, K. Microbial decay of CCAtreated cooling tower timbers. *IAWA Bull.* **1992**, *13*, 215–231. [CrossRef]
23. Singh, A.P.; Wakeling, R.N. Microscopic characteristics of microbial attacks of CCAtreated radiata pine. *Int. Res. Group Wood Preserv.* **1993**. IRG/WP 93-10011. Available online: https://agris.fao.org/agris-search/search.do?recordID=SE9412161 (accessed on 28 September 2021).
24. Lundell, T.K.; Mäkelä, M.R.; de Vries, R.P.; Hildén, K.S. Genomics, lifestyles and future prospects of wood-decay and litter-decomposing basidiomycota. *Adv. Bot. Res.* **2014**, *70*, 329–370. [CrossRef]
25. Singh, A.P.; Kim, Y.S.; Singh, T. Bacterial degradation of wood. In *Secondary Xylem Biology*; Kim, Y.S., Funada, R., Singh, A.P., Eds.; Academic Press: Cambridge, UK, 2016; pp. 169–190.
26. Cufar, K.; Merela, M.; Eric, M. A Roman barge in the Ljubljanica river (Slovenia): Wood identification, dendrochronological dating and wood preservation research. *J. Archaeol. Sci.* **2014**, *44*, 128–135. [CrossRef]

27. Singh, A.; Butcher, J.A. Bacterial degradation of wood cell walls: A review of degradation patterns. *J. Int. Wood Sci.* **1991**, *12*, 43–157.
28. Kim, Y.S.; Singh, A.P.; Nilsson, T. Bacteria as important degraders of waterlogged archaeological woods. *Holzforschung* **1996**, *50*, 389–392. [CrossRef]
29. Daniel, G. Fungal and bacterial biodegradation: White rots, brown rots, soft rots and bacteria. In *Deterioration and Protection of Sustainable Biomaterials*; Schultz, T., Goodell, B., Nicholas, D.D., Eds.; ACS Symposium Series; American Chemical Society: Washington, DC, USA, 2014; pp. 23–56. [CrossRef]
30. Hedges, J.I. The chemistry of archaeological wood. In *Archaeological Wood: Properties, Chemistry, and Preservation*; Rowell, R.M., Barbour, R.J., Eds.; Advances in Chemistry Series 225; American Chemical Society: Washington, DC, USA, 1990; pp. 111–140.
31. Cavallaro, G.; Milioto, S.; Parisi, F.; Lazzara, G. Halloysite Nanotubes loaded with Calcium Hydroxyde: Alkaline Fillers for the Deacidification of Waterlogged Archeological Woods. *ACS Appl. Mater. Interfaces* **2018**, *10*, 27355–27364. [CrossRef] [PubMed]
32. Lisuzzo, L.; Hueckel, T.; Cavallaro, G.; Sacanna, S.; Lazzara, G. Pickering Emulsions Based on Wax and Halloysite Nanotubes: An Ecofriendly Protocol for the Treatment of Archeological Woods. *ACS Appl. Mater. Interfaces* **2021**, *13*, 1651–1661. [CrossRef] [PubMed]
33. Broda, M.; Dąbek, I.; Dutkiewicz, A.; Dutkiewicz, M.; Popescu, C.M.; Mazela, B.; Maciejewski, M. Organosilicons of different molecular size and chemical structure as consolidants for waterlogged archaeological wood a new reversible and retreatable method. *Sci. Rep.* **2020**, *10*, 2188. [CrossRef] [PubMed]
34. Ghavidel, A.; Hosseinpourpia, R.; Militz, H.; Vasilache, V.; Sandu, I. Characterization of Archaeological European White Elm (*Ulmus laevis* P.) and Black Poplar (*Populus nigra* L.). *Forests* **2020**, *11*, 1329. [CrossRef]
35. Rowell, R.M. *Handbook of Wood Chemistry and Wood Composites*; CRC Press: New York, NY, USA, 2012. [CrossRef]
36. EN 15403. *Solid Recovered Fuels—Determination of Ash Content, Supersedes CEN/TS 15403:2006*; CEN: Brussels, Belgium, 2011.
37. Schwarze, F.W.M.R. Wood decay under the microscope. *Fungal Biol. Rev.* **2007**, *21*, 133–170. [CrossRef]
38. Carvalheiro, F.; Duarte, L.C.; Girio, F.M. Hemicellulose biorefineries: A review on biomass pretreatments. *J. Sci. Ind. Res.* **2008**, *67*, 849–864.
39. Han, Y.; Du, J.; Huang, X.; Ma, K.; Wang, Y.; Guo, P.; Li, N.; Zhang, Z.; Pan, J. Chemical Properties and Microbial Analysis of Waterlogged ArchaeologicalWood from the Nanhai No. 1 Shipwreck. *Forests* **2021**, *12*, 587. [CrossRef]
40. Pedersen, N.B.; Łucejko, J.J.; Modugno, F.; Björdal, C. Correlation between bacterial decay and chemical changes in waterlogged archaeological wood analysed by light microscopy and Py-GC/MS. *Holzforschung* **2020**, *75*, 635–645. [CrossRef]
41. Lucejko, J.J.; Tamburini, D.; Zborowska, M.; Babiński, L.; Modugno, F.; Colombini, M.P. Oak wood degradation processes induced by the burial environment in the archaeological site of Biskupin (Poland). *Herit. Sci.* **2020**, *8*, 44. [CrossRef]
42. Crestini, C.; El Hadidi, N.M.N.; Palleschi, G. Characterisation of archaeological wood: A case study on the deterioration of a coffin. *Microchem. J.* **2009**, *92*, 150–154. [CrossRef]
43. Ghavidel, A.; Bak, M.; Hofmann, T.; Vasilache, V.; Sandu, I. Evaluation of some wood-water relations and chemometric characteristics of recent oak and archaeological oak wood (Quercus Robur) with archaeometric value. *J. Cult. Herit.* **2021**, *51*, 21–28. [CrossRef]
44. Capano, M.; Pignatelli, O.; Capretti, C.; Lazzeri, S.; Pizzo, B.; Marzaioli, F.; Martinelli, N.; Gennarelli, I.; Gigli, S.; Terrasi, F.; et al. Anatomical and chemical analyses on wooden artifacts from a Samnite sanctuary in Hirpinia (Southern Italy). *J. Archaeol. Sci.* **2015**, *57*, 370–379. [CrossRef]
45. High, K.E.; Penkman, K.E.H. A review of analytical methods for assessing preservation in waterlogged archaeological wood and their application in practice. *Herit. Sci.* **2020**, *8*, 83. [CrossRef]
46. Daniel, G. Microscope techniques for understanding wood cell structure and biodegradation. In *Secondary Xylem Biology: Origins, Functions, and Applications*; Academic Press: Cambridge, UK, 2016; pp. 309–343.
47. Fengel, D.; Wegener, G. *Wood—Chemistry, Ultrastructure, Reactions*; Walter de Gruyter & Co.: Berlin, Germany, 1989; p. 613.
48. Ljungdahl, L.G.; Eriksson, K.E. Ecology of microbial cellulose degradation. In *Advances in Microbial Ecology*; Marschall, K.C., Ed.; Plenum: New York, NY, USA, 1985; Volume 8.
49. García-Iruela, A.; García Esteban, L.; García Fernández, F.; Palacios, P.; Rodriguez-Navarro, A.B.; Sánchez, L.G.; Hosseinpourpia, R. Effect of Degradation on Wood Hygroscopicity: The Case of a 400-Year-Old Coffin. *Forests* **2020**, *11*, 712. [CrossRef]
50. Popescu, C.-M.; Broda, M. Interactions between Different Organosilicons and Archaeological Waterlogged Wood Evaluated by Infrared Spectroscopy. *Forests* **2021**, *12*, 268. [CrossRef]
51. Hoffmann, P.; Jones, M.A. Structure and degradation process for waterlogged archaeological wood. In *Archaeological Wood*; American Chemical Society: Washington, DC, USA, 1990; pp. 35–65.
52. Ghavidel, A.; Scheglov, A.; Karius, V.; Mai, C.; Tarmian, A.; Vioel, W.; Vasilache, V.; Sandu, I. In-depth studies on the modifying effects of natural ageing on the chemical structure of European spruce (*Picea abies*) and silver fir (*Abies alba*) woods. *J. Wood Sci.* **2020**, *66*, 77. [CrossRef]
53. Gelbrich, J. Bacterial Wood Degradation—A Study of Chemical Changes and Growth Conditions of Bacteria. Ph.D. Thesis, University of Goettingen, Goettingen, Germany, 2009.
54. Highley, T.L.; Murmanis, L.L.; Palmer, J.G. Micromorphology of degradation in western helmlock and sweetgum by the brown-rot fungus, Poria placenta. *Holzforschung* **1985**, *39*, 73–78. [CrossRef]

55. Pettersen, R.C. *The Chemistry of Solid Wood*; Advances in Chemistry Series 20; US Department of Agriculture: Washington, DC, USA, 1984.
56. Cha, M.Y.; Lee, K.H.; Kim, J.S.; Kim, Y.S. Variations in bacterial decay between cell types and between cell wall regions in waterlogged archaeological wood excavated in the intertidal zone. *IAWA J.* **2021**, *1*, 1–18. [CrossRef]